Efficient Photodissociation of Anions from Benzoyl-Functionalized Ferrocene Complexes

Yoshikazu Yamaguchi and Charles Kutal*

Department of Chemistry, University of Georgia, Athens, Georgia 30602

Received February 12, 1999

Spectroscopic and photochemical studies of several benzoyl-functionalized ferrocene complexes in nonaqueous solvents are reported. Bands observed above 300 nm in the electronic absorption spectrum of the unsubstituted complex, Fe(η^5-C_5H_5)$_2$, and assigned to ligand field transitions shift to longer wavelengths and intensify upon introduction of a benzoyl group into one or both cyclopentadienide rings. Such behavior suggests that these transitions have acquired some charge-transfer character. Visible-light (546 nm) irradiation of 1,1′-dibenzoylferrocene, **III**, dissolved in CH_3CN, CH_3OH, or ethyl α-cyanopropionate causes ring−metal cleavage to produce the benzoylcyclopentadienide ion, $C_6H_5C(O)C_5H_4^-$, and the corresponding half-sandwich cationic complex, Fe[(η^5-C_5H_4)$C(O)C_6H_5$](S)$_3^+$ (S is solvent). The disappearance quantum yield, ϕ_{dis}, for **III** is 0.45 in CH_3OH and 0.28 in ethyl α-cyanopropionate and is unaffected by the presence of dissolved O_2, added H_2O (10 000 ppm), or added methanesulfonic acid (30 ppm). 1,1′-Dibenzoylferrocenes containing substitutents on both phenyl rings undergo photoinduced ring−metal cleavage in CH_3OH with ϕ_{dis} values very similar to that of **III**, while monobenzoylferrocenes are appreciably less photoreactive. A mechanism that accommodates the photochemical behavior of benzoyl-functionalized ferrocene complexes is discussed. In addition, a previous suggestion concerning the role of **III** in the photoinitiated anionic polymerization of an α-cyanoacrylate monomer is reconsidered in light of the present study.

Introduction

Ferrocene compounds have been the subject of numerous spectroscopic and photochemical investigations.[1−3] While the parent member of the family, Fe(η^5-C_5H_5)$_2$ (**I** in Figure 1), possesses several potentially reactive ligand field and charge-transfer excited states in the UV−visible spectral region, it is photoinert in nonhalogenated solvents such as cyclohexane, acetone, and methanol. In carbon tetrachloride and other halogenated media, however, **I** forms a photoactive ground-state complex with solvent that is characterized by a charge-transfer-to-solvent (CTTS) absorption band at ∼310 nm. Irradiation of the complex in the wavelength region of this CTTS band causes the one-electron oxidation of **I** to the ferricenium cation and reduction of CCl_4 to its radical anion, an unstable species that promptly dissociates to the $^{\bullet}CCl_3$ radical and Cl^- (eq 1).[4−6] Secondary reactions of these photogenerated species lead to a variety of permanent photoproducts. Acyl-functionalized ferrocenes also exhibit interesting solvent-dependent photochemistry[7] as exemplified by benzoylferrocene (**II** in Figure 1). Reported photoreactions of this compound include aquation of the carbonyl group accompanied by ring−metal and ring−carbonyl cleavage in moist dimethyl sulfoxide (DMSO; eq 2a),[8] ring−metal cleavage without debenzoylation in acidified methanol (eq 2b),[9] and oxidation to the corresponding ferricenium cation in primary alcohols (ROH; eq 2c).[10]

$$\mathbf{I} + CCl_4 \rightleftharpoons \{\mathbf{I},CCl_4\} \xrightarrow{h\nu} \mathbf{I}^+ + Cl^- + {}^{\bullet}CCl_3 \qquad (1)$$

$$\mathbf{II} \xrightarrow{h\nu} \begin{cases} \xrightarrow[H_2O]{DMSO} (\eta^5\text{-}C_5H_5)Fe(DMSO)_n^+ + C_6H_5CO_2^- + C_5H_6 + \mathbf{I} & (2a) \\ \xrightarrow[CH_3OH]{H^+} (\eta^5\text{-}C_5H_5)Fe(CH_3OH)_n^+ + C_6H_5C(O)C_5H_5 & (2b) \\ \xrightarrow{ROH} \mathbf{II}^+ + e^-_{(solv)} & (2c) \end{cases}$$

Ferrocenes have a long history of use as photoinitiators for radical and cationic polymerization reactions.[11,12] Vinyl monomers, for example, polymerize via a $^{\bullet}CCl_3$-initiated pathway when irradiated in CCl_4 solutions containing **I** (see eq 1). In a recent communication, we described the first evidence that ferrocenes also can function as anionic photoinitiators.[13] 1,1′-Dibenzoylferrocene (**III** in Figure 1) was found to be particularly effective as a photoinitiator for the anionic polymerization of an α-cyanoacrylate monomer at wavelengths well into the visible region. Evidence was presented that irradiation of **III** generates a long-lived anion that serves as the active initiating species.

We have continued our investigation of **III** with the goals of identifying the anionic initiating species and elucidating the

(1) Bozak, R. E. *Adv. Photochem.* **1971**, *8*, 227−244.
(2) Warren, K. D. *Struct. Bonding (Berlin)* **1976**, *27*, 45−159.
(3) Geoffroy, G. L.; Wrighton, M. S. *Organometallic Photochemistry*; Academic Press: New York, 1979; Chapter 5.
(4) Traverso, O.; Scandola, F. *Inorg. Chim. Acta* **1970**, *4*, 493−498.
(5) Akiyama, T.; Hoshi, Y.; Goto, S.; Sugimori, A. *Bull. Chem. Soc. Jpn.* **1973**, *46*, 1851−1855.
(6) Akiyama, T.; Sugimori, A.; Hermann, H. *Bull. Chem. Soc. Jpn.* **1973**, *46*, 1855−1859.
(7) Tarr, A. M.; Wiles, D. M. *Can. J. Chem.* **1968**, *46*, 2725−2731.
(8) Ali, L. H.; Cox, A.; Kemp, T. J. *J. Chem. Soc., Dalton Trans.* **1973**, 1468−1475.
(9) Bozak, R. E.; Javaheripour, H. *Chem. Ind. (London)* **1973**, 696−697.
(10) Traverso, O.; Rossi, R.; Sostero, S.; Carassiti, V. *Mol. Photochem.* **1973**, *5*, 457−469.
(11) Allen, D. M. *J. Photograph. Sci.* **1976**, *24*, 61−67.
(12) Yang, D. B.; Kutal, C. In *Radiation Curing; Science and Technology*; Pappas, S. P., Ed.; Plenum Press: New York, 1992; Chapter 2.
(13) Yamaguchi, Y.; Palmer, B. J.; Kutal, C.; Wakamatsu, T.; Yang, D. B. *Macromolecules* **1998**, *31*, 5515−5517.

10.1021/ic990173t CCC: $18.00
Published on Web 09/29/1999

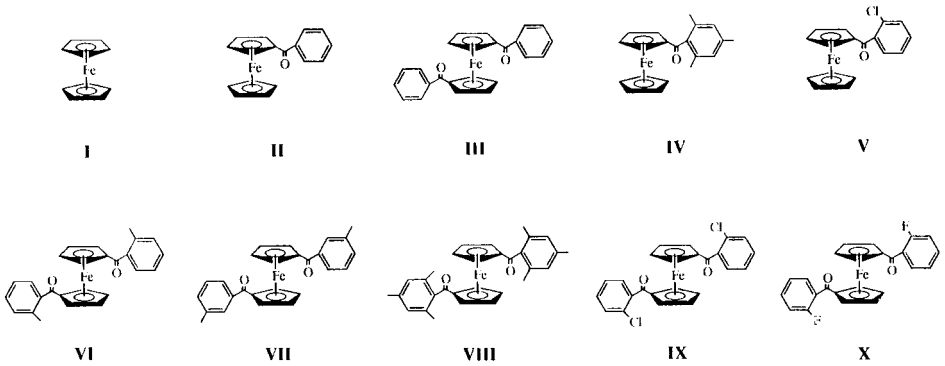

Figure 1. Structures of ferrocenes **I**−**X**.

mechanism of its formation. In addition, we have expanded the range of complexes examined to include several analogues of **II** and **III** (**IV**−**X** in Figure 1) containing substituents on the phenyl rings. Detailed studies of the spectroscopy and photochemistry of this closely related series of acylferrocenes have yielded useful insights concerning the influence of electronic and steric effects on excited-state properties. A full account of our results is presented here.

Experimental Section

A. Materials. Samples of **I** and **II** (both from Aldrich) were further purified by sublimation, while **III** (Sigma) was recrystallized from *n*-hexane. Acid chlorides (Lancaster), ethyl α-cyanopropionate (TCI America), and ethyl α-cyanoacrylate (Loctite) were used as received. Spectral-grade solvents were used without further treatment in the spectroscopic and photochemical experiments.

B. Syntheses of 1,1′-Dibenzoylferrocenes. Compounds **VI**−**X** were prepared by standard Friedel−Crafts acylation of **I** with the corresponding acid chloride.[14,15] All reactions were conducted under an argon atmosphere. The general synthetic procedure will be described in detail for **X**.

1,1′-Bis(*o*-fluorobenzoyl)ferrocene (X). To a two-necked 250-mL round-bottom flask were added 30 mL of CH_2Cl_2 and 1.59 g (10 mmol) of *o*-fluorobenzoyl chloride. The flask was placed in an ice bath and the contents were stirred with a magnetic stirring bar. An orange color developed immediately upon addition of 1.33 g (10 mmol) of $AlCl_3$. After 20 min, 0.78 g (4.25 mmol) of **I** dissolved in 10 mL of CH_2Cl_2 was added via a syringe. The resulting blue-violet solution was stirred for 2 h, whereupon the flask was removed from the ice bath and heated to 30 °C, and the contents were allowed to reflux for 2 days. Analysis of the reaction mixture by thin-layer chromatography (TLC) on silica gel revealed a single product, **X**, characterized by an R_f value of 0.70 with a 2:1 (v:v) mixture of CH_2Cl_2/*n*-hexane as eluant. By comparison, **I** elutes with an R_f of 0.97 under similar conditions. To isolate the product, ∼50 g of ice was added to the flask and the contents were poured into a 1-L separatory funnel containing 500 mL of distilled water. Sufficient NaOH (25 wt % in H_2O) was added to neutralize acid, and the aqueous layer was discarded. The CH_2Cl_2 layer was washed three times with distilled water, transferred to a beaker, and dried by stirring for 20 min with 8 g of anhydrous Na_2SO_4. The dried solution was passed through filter paper and the solvent was removed by vacuum distillation to yield 1.14 g (62%) of a reddish-orange solid. This crude material was recrystallized from warm (∼45 °C) hexane and vacuum-dried overnight. Anal. Calcd for $C_{24}H_{16}F_2O_2Fe$: C, 67.00; H, 3.75. Found: C, 66.77; H, 3.73. mp 152−153.5 °C. ^{1}H NMR (300 MHz, $CDCl_3$): δ 7.00−7.70 (m, 4 H, aromatic), 4.84 (t, 2 H, Cp), 4.63 (t, 2 H, Cp).

1,1′-Bis(*o*-chlorobenzoyl)ferrocene (IX). TLC (CH_2Cl_2): **I**, R_f = 0.94; crude **IX**, R_f = 0.89. Crude yield: 54%, recrystallized from warm *n*-hexane. Anal. Calcd for $C_{24}H_{16}Cl_2O_2Fe$: C, 62.24; H, 3.48. Found: C, 62.32; H, 3.66. mp 163−164 °C. ^{1}H NMR (300 MHz, $CDCl_3$): δ 7.10−7.60 (m, 4 H, aromatic), 4.82 (t, 2 H, Cp), 4.71 (t, 2 H, Cp).

1,1′-Bis(*o*-methylbenzoyl)ferrocene (VI). TLC (CH_2Cl_2): **I**, R_f = 0.98; crude **VI**, R_f = 0.85. Crude yield: 47%, recrystallized from warm *n*-hexane. Anal. Calcd for $C_{26}H_{22}O_2Fe$: C, 73.95; H, 5.25. Found: C, 73.92; H, 5.30. mp 95−96 °C. ^{1}H NMR (300 MHz, $CDCl_3$): δ 7.10−7.70 (m, 4 H, aromatic), 4.80 (t, 2 H, Cp), 4.63 (t, 2 H, Cp), 2.30 (s, 3 H, CH_3).

1,1′-Bis(*m*-methylbenzoyl)ferrocene (VII). TLC (CH_2Cl_2): **I**, R_f = 0.97; crude **VII**, R_f = 0.73. Crude yield: 70%, recrystallized from warm *n*-hexane. Anal. Calcd for $C_{26}H_{22}O_2Fe$: C, 73.95; H, 5.25. Found: C, 73.94; H, 5.31. mp 130.5−131.5 °C. ^{1}H NMR (300 MHz, $CDCl_3$): δ 7.10−7.70 (m, 4 H, aromatic), 4.91 (t, 2 H, Cp), 4.57 (t, 2 H, Cp), 2.41 (s, 3 H, CH_3).

1,1′-Bis(2,4,6-trimethylbenzoyl)ferrocene (VIII). TLC (CH_2Cl_2): **I**, R_f = 0.97; crude **VIII**, R_f = 0.90. Crude yield: 45%, recrystallized from warm *n*-hexane. Anal. Calcd for $C_{30}H_{30}O_2Fe$: C, 75.32; H, 6.32. Found: C, 75.20; H, 6.38. mp 224−226 °C. ^{1}H NMR (300 MHz, $CDCl_3$): δ 6.83 (s, 2 H, aromatic), 4.50−4.80 (m, 4 H, Cp), 2.00−2.50 (m, 9 H, CH_3).

C. Syntheses of Monobenzoylferrocenes. Compounds **IV** and **V** were prepared by a procedure very similar to that described above for **X**. Specific details will be presented for **V**.

***o*-Chlorobenzoylferrocene (V).** To a two-necked 250-mL round-bottom flask were added 20 mL of CH_2Cl_2 and 0.88 g (5 mmol) of *o*-chlorobenzoyl chloride. The flask was placed in an ice bath and the contents were stirred with a magnetic stirring bar. A red-violet color developed immediately upon addition of 0.67 g (5 mmol) of $AlCl_3$. After 20 min, 0.96 g (5.2 mmol) of **I** dissolved in 5 mL of CH_2Cl_2 was added via a syringe. The resulting blue-violet solution was stirred for 3 h, whereupon the flask was removed from the ice bath and the contents stirred for 1 day at 23 °C. Analysis of the reaction mixture by thin-layer chromatography (TLC) on silica gel revealed a single product, **V**, characterized by an R_f value of 0.86 with a 2:1 (v:v) mixture of CH_2Cl_2/*n*-hexane as eluant. The orange product was isolated and purified by the procedures described for **X**. Anal. Calcd for $C_{17}H_{13}ClOFe$: C, 62.91; H,4.04. Found: C, 62.93; H, 4.10. mp 98.5−99.5 °C. ^{1}H NMR (300 MHz, $CDCl_3$): δ 7.30−7.55 (m, 4 H, aromatic), 4.74 (t, 2 H, Cp), 4.59 (t, 2 H, Cp), 4.27 (s, 5 H, Cp).

2,4,6-Trimethylbenzoylferrocene (IV). TLC (CH_2Cl_2): **I**, R_f = 0.97; crude **IV**, R_f = 0.95. Crude yield: 68%, recrystallized from warm *n*-hexane. Anal. Calcd for $C_{20}H_{20}OFe$: C, 72.31; H, 6.07. Found: C, 72.26; H, 6.08. mp 105−108 °C. ^{1}H NMR (300 MHz, $CDCl_3$): δ 6.85 (s, 2 H, aromatic), 4.50−4.70 (m, 4 H, Cp), 4.25 (s, 5 H, Cp), 2.10−2.50 (m, 9 H, CH_3).

Instrumentation. Melting points were determined with a Thomas-Hoover Unimelt apparatus and are uncorrected. Electronic absorption spectra were recorded at room temperature (typically 21 ± 1 °C) on a Varian DMS spectrophotometer. ^{1}H NMR spectra were obtained with a Bruker AC-300 spectrometer. Chemical shifts were referenced to internal tetramethylsilane by assigning the solvent ($CDCl_3$) peak a value of 7.26 ppm.

(14) Mayo, D. W.; Pike, R. M.; Trumper, P. K. *Micro Organic Laboratory*, 3rd ed.; John Wiley: New York, 1994; pp 364−370.
(15) Ranson, R. J.; Roberts, R. M. G. *J. Organomet. Chem.* **1984**, *260*, 307−317.

Electrospray ionization mass spectrometry (ESI MS) experiments were performed on a Perkin-Elmer Sciex API 1 Plus single-quadrupole mass spectrometer. Analyte solutions (20 μL volume) were introduced directly into the spectrometer via an injection loop. The needle and orifice voltages of the ESI source were 4500 and 50−60 V, respectively. Mass resolution was 1 atomic mass unit (amu) for a scan range of 30−200 or 50−1000 amu, a step of 0.2 amu, and a dwell time of 2.0−3.0 ms. Gas chromatography−mass spectrometry (GC−MS) analyses were conducted with a Hewlett-Packard 5890 gas chromatograph interfaced to a Hewlett-Packard 5970 mass selective detector. The gas chromatograph contained a 30 m × 0.25 mm (i.d.) fused silica capillary column (Alltech EC-5) coated internally with a 0.25 μm film of 5% phenyl−95% methylpolysiloxane. Operating temperatures were as follows: injector, 230 °C; column, 3 min at 50 °C, 50−280 °C at 20 °C/min, and 30 min at 280 °C. The flow of helium carrier gas through the column was 0.9 mL/min. The mass detector was scanned over the range 50−550 amu at a rate of 1.3 scans/s.

Continuous photolysis experiments were performed with an Illumination Industries 200-W high-pressure mercury arc lamp. The 546-nm line was isolated with a narrow-band-pass (10 nm at half-height) interference filter, and light intensity at this wavelength was measured with the Reineckate actinometer.[16] Polychromatic light of wavelengths >290 nm was obtained by passing the full output of the lamp through Pyrex glass.

Photochemical Procedures. Solutions of **II**−**X** were irradiated with stirring in 1-cm rectangular quartz cells maintained at 22 ± 1 °C in a thermostated holder. Typical complex concentrations were in the range (1.0−2.5) × 10^{-3} M. The extent of photoreaction was determined spectrophotometrically by monitoring the decrease in intensity of the long-wavelength band (band A) in the electronic absorption spectrum of the complex. The mathematical relationship is given by eq 3, where A_0 is the initial absorbance at the band maximum, A_t is the absorbance after irradiation for time t, and A_f is the final absorbance reached after exhaustive photolysis. Quantum yields were calculated at different extents of reaction (usually <30%) and then linearly extrapolated to zero percent reaction.

$$\% \text{ reaction} = \frac{A_0 - A_t}{A_0 - A_f}(100) \qquad (3)$$

Results and Discussion

Electronic Structure and Spectroscopy. Important features of the electronic structure and spectroscopy of the ferrocenes examined in this study can be understood by examining the qualitative molecular orbital diagram derived for the parent complex, **I** (Figure 2).[2,17] In idealized D_{5d} symmetry, the 10 pπ orbitals of the two cyclopentadienide rings form the symmetry-adapted combinations a_{1g}, a_{2u}, e_{1g}, e_{1u}, e_{2g}, and e_{2u}. Interaction of these ligand orbitals with the metal 3d, 4s, and 4p valence orbitals of appropriate symmetry generates the molecular orbitals characteristic of the complex. The best match in terms of overlap occurs between the ligand e_{1g} set and the $3d_{xz}$,$3d_{yz}$ orbitals. The resulting $1e_{1g}$ molecular orbitals are mostly (∼60%) ligand in character, strongly bonding, and filled with two pairs of electrons, while the corresponding $2e_{1g}$* antibonding orbitals are mainly metal in character and unoccupied. Poor δ-type overlap between the $3d_{x^2-y^2}$,$3d_{xy}$ orbitals and the e_{2g} ring orbitals leads to weak bonding, and, as a consequence, the filled $1e_{2g}$ molecular orbitals retain a large degree (∼90%) of metal character. The near-zero overlap of the $3d_{z^2}$ and ligand a_{1g} orbitals results in a nonbonding molecular orbital, $2a_{1g}$, that is essentially pure metal in composition; this orbital contains two electrons and is the highest occupied level in the complex.

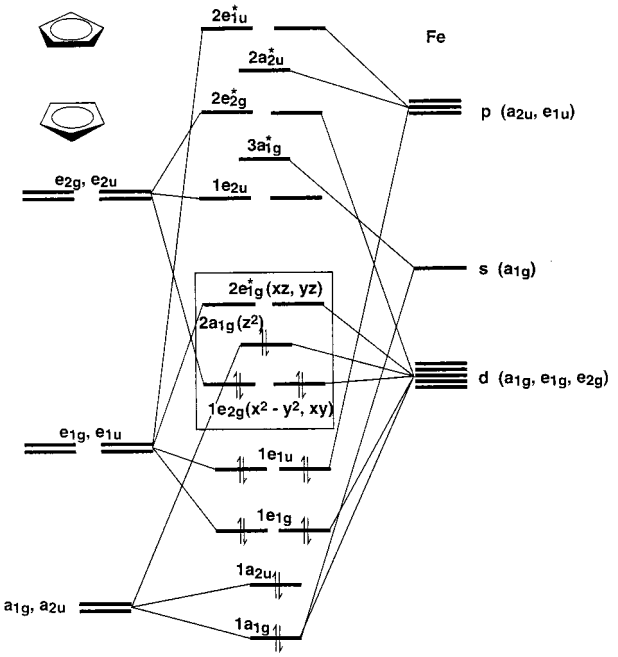

Figure 2. Qualitative molecular orbital diagram for **I**. A box encloses the molecular orbitals that contain appreciable metal d-orbital character.

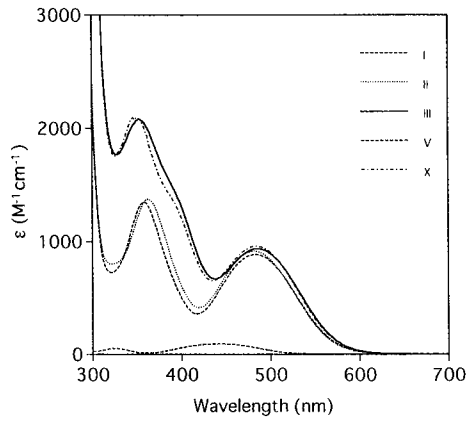

Figure 3. Electronic absorption spectra of several ferrocene complexes in room- temperature methanol.

Since the $1e_{2g}$, $2a_{1g}$, and $2e_{1g}$* molecular orbitals of **I** contain a substantial degree of metal character, the electronic transitions involving these orbitals can be treated within the formalism of ligand field theory.[2,18] The $^1A_{1g}$ ground state of the d^6 complex corresponds to the $(1e_{2g})^4(2a_{1g})^2(2e_{1g}*)^0$ electronic configuration. Photoexcitation of a $2a_{1g}$ electron to the empty $2e_{1g}$* orbitals produces an E_{1g} excited state, while E_{2g} and E_{1g} excited states arise from photoexcitation of a $1e_{2g}$ electron to the $2e_{1g}$* orbitals. Accordingly, three spin-allowed ligand field transitions are expected in the absorption spectrum: $^1A_{1g} \rightarrow a^1E_{1g}$, $^1A_{1g} \rightarrow {}^1E_{2g}$, and $^1A_{1g} \rightarrow b^1E_{1g}$. The first two transitions are unresolved and give rise to the band at 442 nm (band A) in the spectrum of **I** in room-temperature methanol (Figure 3). The third transition is responsible for the band at 325 nm (band B). Consistent with their predominantly ligand field parentage, both bands possess low extinction coefficients and experience only minor changes in position and intensity with variations in solvent polarity (Table 1).

Introduction of an acyl group into one or both cyclopentadienide rings of ferrocene causes an appreciable perturbation

(16) Wegner, E. E.; Adamson, A. W. *J. Am. Chem. Soc.* **1966**, *88*, 394−403.
(17) Clack, D. W.; Warren, K. D. *Struct. Bonding (Berlin)* **1980**, *39*, 1−41.
(18) Sohn, Y. S.; Hendrickson, D. N.; Gray, H. B. *J. Am. Chem. Soc.* **1971**, *93*, 3603−3612.

Table 1. Electronic Absorption Spectral Data for **I**−**X**

		λ_{max}, nm (ϵ, M^{-1} cm^{-1})	
compound	solvent	band A	band B
I	CH_3OH	442 (91.5)	325 (51.3)
I	CP[a]	442 (95.6)	326 (55.1)
I[b]	isooctane	440 (95)	326 (55)
II	CH_3OH	483 (903)	363 (1360)
II	CP	472 (729)	361 (1290)
II	CH_3CN	472 (780)	358 (1340)
II[b]	isooctane	459 (610)	355 (1220)
III	CH_3OH	486 (943)	353 (2090)
III	CP	480 (891)	355 (2200)
III	CH_3CN	480 (885)	353 (2240)
III	cyclohexane	469 (713)	352 (2020)
III[b]	isooctane	470 (700)	354 (1970)
IV	CH_3OH	483 (783)	355 (1360)
V	CH_3OH	483 (885)	358 (1340)
VI	CH_3OH	483 (898)	346 (2080)
VII	CH_3OH	486 (945)	353 (2100)
VIII	CH_3OH	486 (852)	345 (2160)
IX	CH_3OH	486 (915)	347 (2170)
IX	cyclohexane	473 (672)	346 (1900)
X	CH_3OH	484 (963)	349 (2180)

[a] CP, ethyl α-cyanopropionate. [b] Data from ref 7.

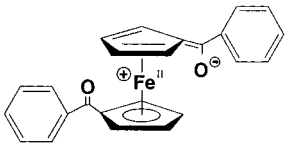

Figure 4. Resonance structure representing the charge-transfer character that results from conjugation between the cyclopentadienide ring and the carbonyl group of electronically excited **III**. The oxidation state of the metal is indicated by a Roman numeral, while formal charges on atoms are circled.

of the absorption spectrum. As seen in Figure 3 and Table 1, bands A and B in the spectra of **II**−**X** appear at longer wavelengths and with substantially higher intensities than their counterparts in the spectrum of **I**. Previous workers have attributed this behavior to conjugation between the five-membered ring and the adjacent carbonyl group in the photoexcited acyl-functionalized complexes.[7,10] Expanding upon this general idea, we propose that conjugation introduces some charge-transfer character into the $^1A_{1g} \rightarrow a^1E_{1g}$, $^1A_{1g} \rightarrow {}^1E_{2g}$, and $^1A_{1g} \rightarrow b^1E_{1g}$ transitions of **II**−**X** (for ease of comparison to **I**, we assume effective D_{5d} symmetry for these complexes). Each of these transitions involves the promotion of an electron to the $2e_{1g}$* molecular orbitals, which, although predominantly metal-based, contain some cyclopentadienide ring π-orbital character. Conjugation of these ring orbitals with the π orbitals of the adjacent C═O group can be represented by a resonance structure of the type drawn for **III** in Figure 4.[19] Here the formal charges on the iron and carbonyl oxygen connote a shift of electron density from the metal to the ligand. This charge-transfer character should stabilize the a^1E_{1g}, $^1E_{2g}$, and b^1E_{1g} excited states relative to the ground state in polar media. In agreement with this expectation, band A in the spectra of the acyl ferrocenes undergoes a substantial shift to longer wavelengths when the solvent is switched from a hydrocarbon to methanol (Table 1). The much smaller shift observed for band

(19) An analogous resonance structure can be drawn for the charge-transfer transition occurring in benzophenone containing a strong electron-releasing group (e.g., NH_2) in the *para* position of a phenyl ring. See Turro, N. J. *Modern Molecular Photochemistry*; Benjamin/Cummings Publishing Co.: Menlo Park, CA, 1978; p 376.

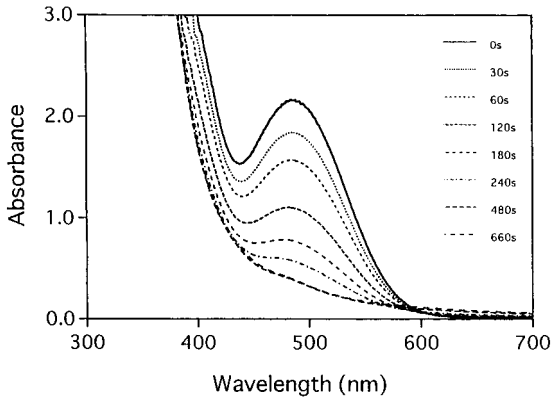

Figure 5. Spectral changes resulting from the 546-nm photolysis of **III** in CH_3OH. Light intensity was 1.22×10^{-7} einstein/s; irradiation times are indicated in the legend.

B suggests less charge-transfer character in the $^1A_{1g} \rightarrow b^1E_{1g}$ transition and/or the overlapping of this transition by other electronic transitions (e.g., note a shoulder at ∼300 nm in the spectra of **III** and **X** shown in Figure 3) having a smaller or opposite response to changes in solvent polarity.[7]

The foregoing analysis of the spectral properties of **I**−**X** has led to the proposal that acyl substitution on the cyclopentadienide ring(s) of ferrocene introduces a degree of charge transfer into some of the electronic transitions responsible for the absorption bands observed above 300 nm. We turn now to the results of photochemical studies that indicate this charge-transfer character also influences the excited-state reactivity of these complexes.

Photochemistry. Early qualitative studies by Tarr and Wiles[7] established that **III** undergoes photodecomposition in a broad range of organic solvents. We repeated some of this work in an effort to find a suitable solvent for the identification of photoproducts and the determination of quantum yields. Irradiation of the complex at 546 nm in air-saturated CH_3CN caused the rapid (2−3 min) formation of a dark-brown precipitate that scattered the incident light and thereby precluded accurate quantum yield measurements. Addition of 2,2′-bipyridine (bipy) to the photolyte after filtering off the precipitate did not produce the characteristic red color of $Fe(bipy)_3^{2+}$, indicating that little Fe^{2+} was present in solution. The precipitate was insoluble in *n*-hexane, acetone, methanol, ethanol, and water but dissolved in 12 N hydrochloric acid and 88% formic acid. Elemental analysis revealed a low C/H/N content (C, 19.06%; H, 2.50%; N, 0.57%), suggesting that the solid consists mainly of inorganic iron (presumably oxides).

Somewhat different behavior occurred upon irradiating **III** in air-saturated CH_3OH or ethyl α-cyanopropionate (abbreviated CP). The solutions acquired a brownish hue as photolysis proceeded but remained homogeneous over at least the initial 33% of the photoreaction. Band A steadily decreased in intensity, while the absorbance increased sharply at shorter wavelengths (Figure 5). An extensively photolyzed solution of **III** in CH_3OH deposited a dark-brown precipitate that was appreciably richer in carbon (C, 47.91%; H, 3.38%; N, 0.0%) than the solid isolated from CH_3CN. After removal of this precipitate by filtration, the filtrate gave a negative test for Fe^{2+} upon addition of 2,2′-bipyridine. In contrast, an extensively irradiated solution of **III** in CP, from which little precipitation had occurred, tested positively for Fe^{2+}. Irradiation of **III** in argon-saturated CP (similar behavior occurred in CH_3OH) initially produced a light-yellow solution that, in the dark, quickly turned brown upon exposure to air. Moreover, the final

Table 2. GC−MS Analytical Data

run	compound[a]	formula weight	λ_{ex},[b] nm	irrdn time, s	GC retention time, min	MS peaks *m/e*, amu
1	**II**	290.15			15.7	290
2	**II**		546	4500	1.5	66[c]
					11.2	170, 105, 77, 65[d]
					15.7	290
3	**II**		>290	180	1.5	66[c]
					11.2	170, 105, 77, 65[d]
					15.7	290
4	**III**	394.26			27.6	394
5	**III**		546	1450[e]	11.2	170, 105, 77, 65[d]
6	**III**		365	180	11.2	170, 105, 77, 65[d]
					27.8	394
7	**III**		>290	10	11.2	170, 105, 77, 65[d]
					27.8	394
8	**X**	430.23			26.6	430
9	**X**		546	480	11.2	188, 123, 95, 65[f]

[a] Initial concentration: 2.0×10^{-3} M. [b] Photoexcitation wavelength. [c] Assignment: 66 amu ($C_5H_6^+$). [d] Assignments: 170 amu [$C_6H_5C(O)C_5H_5^+$], 105 amu [$C_6H_5C(O)^+$], 77 amu ($C_6H_5^+$), 65 amu ($C_5H_5^+$). [e] Photolyte filtered through 0.2 μm PTFE filter prior to analysis. [f] Assignments: 188 amu [*o*-(C_6H_4F)$C(O)C_5H_5^+$], 123 amu [*o*-(C_6H_4F)$C(O)^+$], 95 amu ($C_6H_4F^+$), 65 amu ($C_5H_5^+$).

absorption spectrum of the photolyte closely matched that of an identically irradiated air-saturated sample. These observations indicate that one or more of the photoproduct(s) can react with O_2.

Further characterization of the photoproducts was facilitated by the use of mass spectrometry. Table 2 contains a summary of GC−MS data for several compounds considered in the ensuing discussion. The mass spectrum of **III** exhibits a prominent parent ion peak at *m/e* = 394 amu (run 4). Photolysis of the complex in CH_3OH over a wide wavelength range generated a single detectable non-metal-containing product assigned as benzoylcyclopentadiene, $C_6H_5C(O)C_5H_5$ (runs 5−7). The concentration of this photoproduct decreased to ~40% of its initial value upon storage of the photolyte in the dark for 4 days. As noted earlier, a dark-brown solid precipitated from solution over the same time period. Electrospray ionization mass spectrometry was used to analyze the photolyte obtained upon irradiation of **III** in CH_3CN at 546 nm for 38 s followed by filtration to remove the precipitate. Major peaks observed at *m/e* values of 171 and 348 amu correspond to protonated benzoylcyclopentadiene and the cationic iron(II) complex $Fe[(\eta^5\text{-}C_5H_4)C(O)C_6H_5](CH_3CN)_3^+$, respectively. Dissolution of the precipitate in 88% formic acid and analysis of the resulting solution by ESI MS revealed a complex mixture of iron-containing products. While we were unable to identify all species present in the mixture, Fe^{2+} complexes containing formate and benzoate were evident.

We conclude from the analytical data summarized above that the primary photochemical reaction of **III** is heterolytic dissociation of the benzoyl-substituted cyclopentadienide ion, **XI,** with the accompanying production of the half-sandwich iron(II) complex, **XII** (eq 4; S is solvent). Both of these photogenerated species undergo further reactions that yield the observed products. Protonation of **XI** by solvent or adventitious traces of water produces the corresponding benzoylcyclopentadiene,[20] which was identified by GC−MS. Thermal and/or photochemical decomposition of **XII** releases Fe^{2+}, which was detected as its colored complex with 2,2′-bipyridine. Other processes available to the photoproducts include reaction with oxygen and precipitation from solution. Because of this complicated series of secondary reactions, the final compositions of the liquid photolyte and any solid precipitate will vary with experimental conditions (e.g., nature of solvent, O_2 concentration, storage time before analysis).

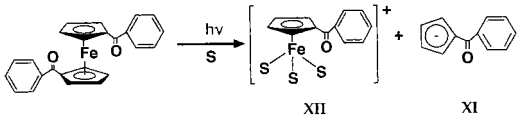

(4)

Table 3 contains a summary of disappearance quantum yield (ϕ_{dis}) data for **III** (runs 3−7). These values were determined by monitoring the photoinduced decrease in intensity of the long-wavelength absorption band of the complex (Figure 5) as described in the Experimental Section. Since the absorption spectra of the primary photoproducts, **XI** and **XII** in eq 4, are not available, the quantum efficiency of ring−metal cleavage (ϕ_{cl}) cannot be determined directly. However, if this process is the sole (or dominant) primary photoreaction of **III**, as suggested by the analytical results, then $\phi_{cl} \geq \phi_{dis}$. Consequently, the data in Table 3 support the conclusion that heterolytic cleavage of a benzoyl-functionalized cyclopentadienide ring occurs with high quantum efficiency upon irradiation with visible (546 nm) light. Solvent plays a role in this process as evidenced by the ~40% decrease in ϕ_{dis} that results upon switching from CH_3OH to CP (runs 3 and 7). In contrast, ϕ_{dis} is rather insensitive to added H_2O (run 5), added methanesulfonic acid (run 6), and dissolved O_2 (run 4). This latter observation indicates that, while O_2 can react with one or more photoproduct(s), it does not influence the efficiency of the primary photochemical reaction.

Photochemical studies of other 1,1′-dibenzoylferrocenes were conducted in CH_3OH, since this solvent proved to be well suited for product analyses and quantum yield measurements. Visible-light irradiation of **VI**−**X** caused spectral changes very similar to those observed for **III** (Figure 5), and the resulting ϕ_{dis} values for the entire set of complexes fall within a narrow range (runs 3 and 9−13 in Table 3). GC−MS analysis of a photolyzed solution of **X** established that *o*-fluorobenzoylcyclopentadiene, *o*-(C_6H_4F)$C(O)C_5H_5$, is a major photoproduct (Table 2, run 9). These results indicate that **VI**−**X**, like **III**, undergo efficient

Table 3. Disappearance Quantum Yield (ϕ_{dis}) Data

run[a]	compound	ϕ_{dis}[b]
1	**II**	0.083
2	**II**[c]	0.035
3	**III**	0.45
4	**III**[d]	0.42 ± 0.06
5	**III**[e]	0.42
6	**III**[f]	0.39
7	**III**[c]	0.28
8	**V**	0.098
9	**VI**	0.41 ± 0.02
10	**VII**	0.41 ± 0.02
11	**VIII**	0.34 ± 0.00
12	**IX**	0.41 ± 0.01
13	**X**	0.47 ± 0.02

[a] Experimental conditions: excitation wavelength, 546 nm; light intensity, $(1.1 \pm 0.1) \times 10^{-7}$ einstein/s; temperature, 22 ± 1 °C; solvent, CH_3OH unless indicated otherwise. [b] Where quoted, error limit represents mean deviation of two runs. Estimated accuracy of ϕ_{dis} is 10−15%. [c] Solvent is ethyl α-cyanopropionate (CP). [d] Purged with argon for 30 min prior to irradiation. [e] Contains 1.0 wt % H_2O. [f] Contains 30 ppm methanesulfonic acid.

(20) Cyclopentadienide ions should be sufficiently basic to remove a proton from methanol or water. See Lowry, T. H.;, Richardson, K. S. *Mechanism and Theory in Organic Chemistry*; Harper and Row: New York, 1976; p 40.

photodissociation of a benzoyl-substituted cyclopentadienide ion (analogous to eq 4) in solution.

While fewer experiments were conducted on the monobenzoylferrocenes, **II**, **IV**, and **V**, the available evidence again points to heterolytic ring-metal cleavage (eq 5; S is solvent) as the primary photoreaction. Thus, an irradiated and filtered solution of **V** tested positively for Fe^{2+} upon addition of 2,2′-bipyridine, while GC−MS analysis established that cyclopentadiene, C_5H_6, and benzoylcyclopentadiene are produced during the photolysis of **II** (Table 2, runs 2 and 3). Data in Table 3 reveal that **II** (run 1) and **V** (run 8) possess similar ϕ_{dis} values in CH_3OH, and ϕ_{dis} decreases upon switching the solvent from CH_3OH to CP (runs 1 and 2). These results also confirm the qualitative observation of Tarr and Wiles[7] that monoacylferrocenes are appreciably less photosensitive than their 1,1′-diacylferrocene analogues (compare **II** vs **III**, **V** vs **IX**).

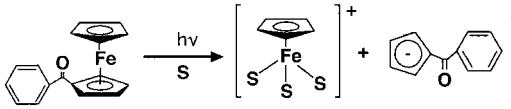

(5)

Mechanistic Considerations. It will be useful at the outset of this discussion to review the various mechanisms proffered by previous workers to account for photoinduced ring-metal cleavage in acylferrocene complexes. Tarr and Wiles[7] suggested that irradiation of **III** in CH_3OH initially causes the transfer of an electron from the complex to the solvent:

$$\mathbf{III} \xrightarrow[CH_3OH]{h\nu} \mathbf{III}^+ + {}^{\bullet}CH_3 + OH^- \qquad (6)$$

Reaction between the resulting ferricenium ion, $\mathbf{III}^+$, and a solvent-derived methyl radical then leads to breakdown of the ring−metal bonding. We can discount the operation of a radical-mediated mechanism in our systems on grounds that O_2, an effective radical scavenger, does not influence the quantum efficiency of the photoreaction (Table 3, runs 3 and 4). In their study of acylferrocene photochemistry in strongly acidic solutions, Bozak and Javaheripour[9] proposed that the metallocene complex is protonated at the acyl oxygen atom in the ground state and that this species undergoes heterolytic photodissociation of a cyclopentadienide ligand. Since the solvent media typically employed in our work did not contain a strong proton donor, we also can discount a mechanism that involves protonation of the ferrocene complex prior to the primary photochemical step. Last, Kemp and co-workers[8] concluded that the photoproducts obtained upon photolysis of acylferrocenes in moist solvents results from the photoaquation of the carbonyl moiety followed by both ring−metal and ring−carbonyl cleavage (eq 2a). Our observation that 1,1′-dibenzoylferrocenes undergo highly efficient photodissociation of an *intact* benzoyl-substituted cyclopentadienide ion (eq 4) indicates that ring−metal cleavage precedes any process involving fission of this ligand.

Scheme 1 outlines a mechanism that accommodates the present results on the solution photochemistry of **III** and related benzoyl-functionalized ferrocenes and, more generally, provides a framework for understanding many of the observations reported in earlier photochemical studies of acylferrocene complexes.[7−9] Absorption of 546-nm light by the complex occurs in the region of band A (Figure 3), which, as noted previously, contains overlapping contributions from the $^1A_{1g} \rightarrow a^1E_{1g}$ and $^1A_{1g} \rightarrow {}^1E_{2g}$ ligand field transitions. Both transitions place electron density in the strongly antibonding $2e_{1g}$* molecular orbitals, thereby weakening ring−metal bonding, while

Scheme 1

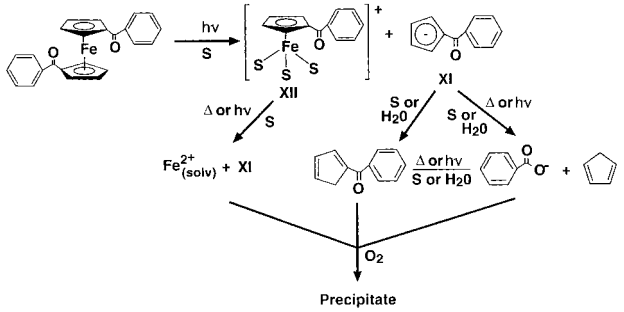

creating an energetically low-lying vacancy in the $3d_{z^2}$ or $3d_{x^2-y^2}$,$3d_{xy}$ orbitals (Figure 2) that facilitates nucleophilic attack on the metal by the solvent. In addition, we have argued that ligand field excited states in acylferrocenes contain a degree of charge-transfer character that, as represented by the resonance structure in Figure 4, results in reduced hapticity ($\eta^5 \rightarrow \eta^4$) of a five-membered ring and a formal positive charge on the metal center. This photoinduced charge-transfer thus reinforces the labilization of ring−metal bonding and the susceptibility of the metal center to nucleophilic attack. Consequently, photoexcited **III** is favorably disposed to undergo loss of the benzoyl-substituted cyclopentadienide ion, **XI**, with the concomitant production of the half-sandwich iron(II) complex, **XII**. While not required by our results, it seems reasonable to suggest that this process occurs via one or more ring-slipped intermediates containing coordinated solvent;[21] one possible example is $[(\eta^5\text{-}C_5H_4)C(O)C_6H_5)]Fe[(\eta^3\text{-}C_5H_4)C(O)C_6H_5)]S^+$. Such species have the option of reacting further with solvent to yield **XII** or expelling coordinated solvent to regenerate the parent complex. The varying abilities of different solvents to compete with the labilized ring for coordination sites about the metal provides a ready explanation for the solvent-dependent photosensitivity of acylferrocenes reported by Tarr and Wiles[7] and our observation of solvent-dependent ϕ_{dis} values (Table 3).

Secondary photochemical and/or thermal reactions of **XI** and **XII** can occur to yield the variety of photoproducts observed in different studies. Loss of a benzoyl-substituted cyclopentadienide ion from **XII** produces solvated Fe^{2+}, which, depending upon the experimental conditions, may undergo additional reactions including oxidation by O_2 and precipitation. Protonation of **XI** yields neutral benzoylcyclopentadiene, while aquation of the C=O group and ring−carbonyl cleavage afford benzoate ion and a cyclopentadiene molecule. We suspect that the latter products, which were detected by Kemp et al.[8] in samples of **II** (eq 2a) irradiated for long times at short wavelengths, arise from the secondary photolysis of **XI** or its protonated offspring.

Data in Table 3 reveal that substituents on the phenyl ring do not greatly influence the quantum efficiency of ring−metal cleavage in monobenzoylferrocene and 1,1′-dibenzoylferrocene complexes.[22]The electron-withdrawing fluorine atoms in **X** enhance ϕ_{dis} relative to the electron-releasing methyl groups in **VI** (runs 9 and 13), but the effect is not large. Steric effects also may contribute to the smaller ϕ_{dis} value for **VIII** (run 11), since this is the only complex that provides two *ortho* substit-

(21) For examples of photoinduced ring-slippage of cyclopentadienide rings, see Dunwoody, N.; Lees, A. J. *Organometallics* **1997**, *16*, 5770−5778.

(22) For a discussion of substituent effects on the photosubstitution reactions of $Fe(\eta^5\text{-}C_5H_5)(\eta^6\text{-arene})^+$ complexes, see Schrenk, J. L.; McNair, A. M.; McCormick, F. B.; Mann, K. R. *Inorg. Chem.* **1986**, *25*, 3501−3504.

uents on each phenyl ring for shielding the metal from nucleophilic attack by solvent.

Our results on the solution photochemistry of benzoylferrocenes compare well with those reported by previous workers with one notable exception. We find that 546-nm irradiation of **II** in CH_3OH leads to heterolytic ring−metal cleavage as the primary photochemical process (eq 5), whereas Traverso et al.[10] concluded that photoexcitation in the wavelength range 313−436 nm results in the photooxidation of **II** to the corresponding ferricenium ion (eq 2c). Because different wavelength regions were employed in the two studies, one possible explanation for the disparity in photochemical behavior is the involvement of two photoactive excited states, a low-energy ligand field state leading to ring−metal labilization and a higher-energy CTTS state resulting in solvated electron production. Notwithstanding this possibility, we are puzzled by the absence in the earlier investigation of any ring−metal cleavage upon excitation at 436 nm, since this wavelength falls within band A of **II** and thus should be effective in exciting a ligand field transition. Further mechanistic studies of this system appear to be warranted.

Concluding Remarks. The mechanism by which **III** functions as a photoinitiator for the anionic polymerization of ethyl α-cyanoacrylate (abbreviated CA) can be revisited in light of the present results. Previously, we reported[13] that irradiation of the complex dissolved in neat CA releases an anionic species X^- that adds to the carbon−carbon double bond of the monomer to yield a resonance-stabilized carbanion (eq 7). Polymerization then proceeds rapidly via the repetitive addition of monomer units to the growing anionic chain. Lacking positive identification of X^-, we suggested that it might be benzoate ion on the basis of the earlier work of Kemp et al.[8] We now know that **III** can undergo highly efficient photodissociation of an intact benzoyl-substituted cyclopentadienide carbanion, **XI** (eq 4). Consequently, **XI** can play the role of the initiating species in the anionic polymerization of CA.

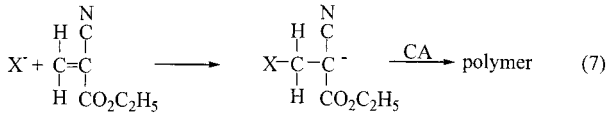

(7)

Ferrocenes **VI**−**X** also are highly effective photoinitiators for the anionic polymerization of CA. Quite interestingly, the presence of *ortho* substituents on the phenyl rings enhances the thermal stability of a complex (relative to **III**) in the monomer solution, thereby lengthening the effective shelf life of the resulting photosensitive formulation. Our detailed studies of this promising new series of anionic photoinitiators will be described in a forthcoming article.

Acknowledgment. We appreciate the technical assistance provided by Dr. Dennis Phillips (mass spectrometry experiments) and Dr. Quincy Teng (NMR measurements). Financial support for this work was received from the JSR Corporation.

IC990173T